Proceedings of the
44th IEEE Conference on Decision and Control, and
the European Control Conference 2005
Seville, Spain, December 12-15, 2005

Sensor-less Vibration Suppression and Scan Compensation for Piezoelectric Tube Nanopositioners

(Invited Paper)

Andrew J. Fleming and S. O. Reza Moheimani

***Abstract*— Piezoelectric tube scanners are employed in high-resolution positioning applications such as scanning probe microscopy and nano-fabrication. Much research has proceeded with the aim of reducing hysteresis and vibration, the foremost problems associated with piezoelectric tube scanners. In this paper, two simple techniques are proposed for simultaneously reducing hysteresis and vibration. Experimental results demonstrate significant reduction in hysteresis due to the use of a charge amplifier. Previous problems involved with the implementation of such amplifiers are resolved to provide DC accurate performance with zero voltage drift. Secondly, piezoelectric shunt damping, a technique previously resident in the field of smart structures, is applied to damp tube vibration. By attaching an LCR impedance to a single tube electrode, the first mechanical mode is reduced in magnitude by more than 20 dB.**

I. Introduction

Piezoelectric tube scanners were first reported in [1] for use in scanning tunneling microscopes. They were found to provide a higher positioning resolution and greater bandwidth than traditional tripod positioners whilst being simple to manufacture and easier to integrate into a microscope. Piezoelectric tube scanners are now used extensively in scanning probe microscopes and many other applications requiring precision positioning e.g. nanomachining [2], [3] etc.

A piezoelectric scanner comprises a tube of radially poled piezoelectric material, four external electrodes, and a grounded internal electrode. Other configurations may include: a circumferential electrode for independent vertical extension or diameter contraction, and/or sectored internal electrodes. Small-deflection expressions for the lateral tip translation, derived from the IEEE Piezoelectricity Standard [4], can be found in [5].

The foremost difficulties associated with piezoelectric tube scanners are the low mechanical resonance frequency, and hysteresis [6]. Techniques aimed at addressing both mechanical dynamics and hysteresis can be grouped generally into two broad categories, feedforward and feedback. Feedforward techniques, do not include a sensor but require accurate knowledge of the undesirable dynamics. Feedback systems, although more robust to modeling error, are limited by the noise performance and bandwidth of the sensor. In many cases it is also difficult and/or prohibitively expensive to integrate displacement sensors into the scanning apparatus.

Considering the breadth of research aimed at improving scan performance, it is surprising to find that commercial microscope manufacturers have been reluctant to adopt any sophosticated techniques. The majority of commercial scanning systems operate in much the same fashion as they did in the early 90's. Regardless of the potential benefits, the requirement for data acquisition, sophisticated modeling experiments, and additional sensors have severely limited the application of feedforward and feedback scan compensation. With this in mind, the research presented in this paper introduces two simple non-model based techniques for the reduction of hysteresis and vibration.

Both authors are with the School of Electrical Engineering and Computer Sciece, University of Newcastle, Callaghan 2308, Australia andrew.fleming@newcastle.edu.au

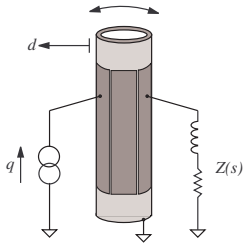

Fig. 1. Charge driven tube scanner with piezoelectric shunt damping circuit.

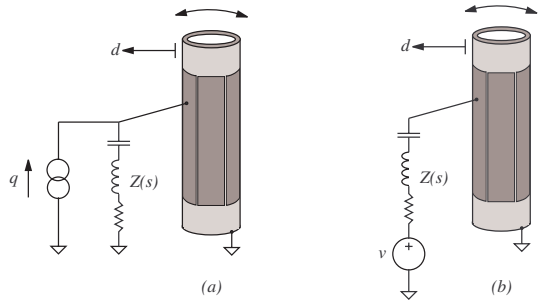

Fig. 2. (a) Charge driven tube scanner. (b) Voltage equivalent circuit.

Since the late 80's, it has been known that driving piezoelectric transducers with current or charge rather than voltage significantly reduces hysteresis [7]. Simply by regulating the current or charge, a five-fold reduction in the hysteresis can be achieved [8]. A quote from a recent paper [9] typifies the sentiment toward this technique, "While hysteresis in a piezoelectric actuator is reduced if the charge is regulated instead of the voltage [7], the implementation complexity of this technique prevents a wide acceptance [10]".

The first contribution of this paper is to present a new class of grounded-load charge amplifier free from DC and low-frequency voltage drift. The second contribution is a new technique for the reduction of scan induced and exogenous vibration. Drawn from the field of Smart Structures, we propose the connection of an electrical impedance to the terminals of one x and y electrode. Usually referred to as piezoelectric shunt damping, this technique results in a damped electrical resonance capable of significantly reducing the magnitude of one or more structural modes. Figure 1 illustrates an inductor and resistor connected to the terminals of a charge driven piezoelectric tube. In this configuration, the inductor and resistor are tuned to damp the first x axis cantilever mode. Undesired resonance excitation due to scanning and external disturbance is attenuated.

Piezoelectric shunt damping requires no feedback sensor

0-7803-9568-9/05/$20.00 ©2005 IEEE

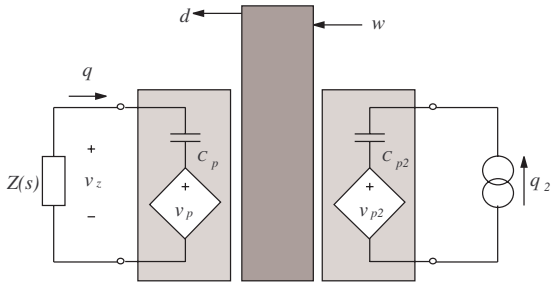

Fig. 3. The electrical equivalent of a charge driven piezoelectric tube with attached shunt circuit.

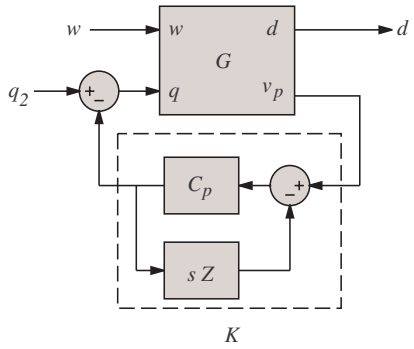

Fig. 4. The equivalent feedback diagram representing an electrical impedance connected to the terminals of one tube electrode. The other electrode is driven with charge.

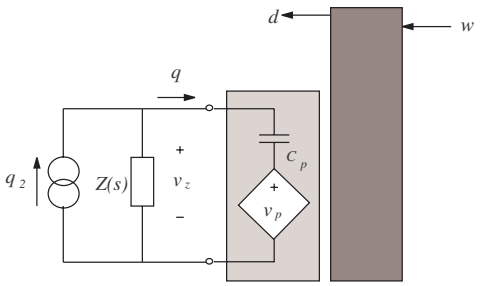

Fig. 5. The electrical equivalent of a piezoelectric tube with charge drive and shunt circuit connected to the same electrode

and is thus immune to the usual problems of low-bandwidth and measurement noise associated with optical and capacitive sensors. Furthermore, as illustrated in Figure 2, we demonstrate that the shunt impedance $Z(s)$, can be applied to the same electrode as the driving charge or voltage source. This allows the redundant electrode to be used for increasing the scan range or as a piezoelectric strain sensor.

In Section 2, we discuss the modeling of a piezoelectric tube and analyze the effect of a connected shunt impedance. Implementation issues are then discussed in Section 3, followed by experimental results and conclusions in Sections 4 and 5.

II. Shunt Circuit Modeling

Although first appearing in [11], the concept of piezoelectric shunt damping is mainly attributed to Hagood and von Flotow [12]. A series inductor-resistor network, as shown in Figure 1, was demonstrated to significantly reduce the magnitude of a single structural mode. Together with the inherent piezoelectric capacitance, the network is tuned to the resonance frequency of a single structural mode. Analogous to a tuned mechanical absorber, additional dynamics introduced by the shunt circuit act to increase the effective structural damping [12].

A. Two Electrode Case

The equivalent electrical model of a shunted piezoelectric tube (as shown in Figure 1) is illustrated in Figure 3. To find the transfer function relating displacement d to the driving charge q_2 we begin by writing Kirchoff's Voltage Law around the impedance loop and substituting $v_z = -qsZ(s)$,

$$\frac{-q(s)}{C_p} - v_p(s) + -q(s)sZ(s) = 0. \tag{1}$$

When the opposing tube electrodes are equal in dimension, the charges q and q_2 have an equal but opposite influence on the tube deflection d and v_p. Furthermore $v_p = -v_{p2}$. We define the transfer functions relating the applied charge to the resulting piezoelectric voltage and tip displacement as $G_{vq}(s)$ and $G_{dq}(s)$. Due to the system symmetry, $G_{vq}(s)$ can be used to relate the following signals:

$$\frac{v_p(s)}{q(s)} = \frac{v_{p2}(s)}{q_2(s)} = \frac{-v_p(s)}{q_2(s)} = G_{vq}(s) \tag{2}$$

The principle of superposition can be applied to find an expression for v_p.

$$v_p(s) = G_{vq}(s)q(s) - G_{vq}(s)q_2(s). \tag{3}$$

Rearranging (3) in terms of q_2 and substituting into (1) yields

$$\frac{v_p(s)}{q_2(s)} = \frac{-G_{vq}(s)}{1 + G_{vq}(s)K(s)} \tag{4}$$

where

$$K(s) = \frac{C_p}{1 + C_p sZ(s)}. \tag{5}$$

The shunted displacement transfer function can be derived in a similar manner,

$$\frac{d(s)}{q_2(s)} = \frac{G_{dq}(s)}{1 + G_{vq}(s)K(s)} \tag{6}$$

From Equation (6) it is concluded that the presence of an electrical shunt impedance can be viewed equivalently as a strain-voltage feedback control system. A diagrammatic representation of equation (6) is shown in Figure 4. Further interpretation and analysis can be found in [13].

B. Hybrid Operation

As mentioned in the introduction, it is advantageous to connect the shunt impedance and charge source to the same electrode. In this subsection, the electrical filtering effect of $Z(s)$ on q_2 is derived. If such a filtering effect can be inverted, the charge source q_2 can be used for scanning, analogous to the case where a shunt impedance is attached to an independent electrode.

Writing Kirchoffs Voltage Law around the loop,

$$-\frac{q}{C_p} - v_p + v_z = 0, \tag{7}$$

and substituting the following,

$$q(s) = -\frac{v_z(s)}{sZ(s)} + q_2(s), \tag{8}$$

results in the loop equation

$$-\frac{q(s)}{C_p} - v_p(s) + q(s)sZ(s) + q_2(s)sZ(s) = 0. \tag{9}$$

Given that $v_p = G_{vq}q$, we can substitute $q = v_p/G_{vq}$ into (9). After simplification, the transfer function from q_2 to v_p can be found:

$$\frac{v_p(s)}{q_2(s)} = \frac{K(s)Z(s)G_{vq}(s)}{1 + G_{vq}(s)K(s)},$$

where K is as given in (5). Similarly,

$$\frac{d(s)}{q_2(s)} = \frac{K(s)Z(s)G_{dq}(s)}{1 + G_{vq}(s)K(s)}. \tag{10}$$

Unlike the two-electrode case, the impedance $Z(s)$ distorts the tube transfer function from the driving charge q_2 to the deflection d. Rather than simply adding a strain feedback controller to the mechanical system, the transfer function from q_2 to d now contains a filter $F(s) = K(s)Z(s)$.

An obvious technique for recovering the natural tube dynamics is to pre-filter the driving charge with $F^{-1}(s)$. Fortunately this pre-filtering and inversion is straight-forward to implement in practice. This solution is discussed in Section III.

C. Shunt Impedance Design

The Smart Structures and Vibration Control literature contains a multitude of passive, active, linear, and non-linear piezoelectric shunt impedance designs (reviewed in [14], [15]). Only a small subset of techniques are suitable for piezoelectric tube damping. The so-called resonant linear shunts meet all of the requisite criteria, primarily, they are easy to design, implement and tune, they offer excellent damping performance (especially for single modes of vibration), they are strictly passive and inject no harmonics, and finally, their presence influences the mechanical dynamics only over a small frequency range. Resonant linear shunts have been shown to emulate the effect of a tuned-mass mechanical absorber [12]. After examining various impedance designs, the LCR circuit depicted in Figure 2 was found to offer good performance. The presence of a series capacitance is necessitated by the requirement for DC tracking. If the impedance of the network was not infinity at DC, constant tube deflections would require a ramp signal in charge (eventually saturating the amplifier), this is reflected in the scan filter $F(s)$ and its inverse $F(s)^{-1}$

To damp a single mode of structural vibration, the circuit inductance L, capacitance C, and piezoelectric capacitance C_p are tuned to resonate at the target mechanical frequency ω_1. Although the capacitance value C is essentially arbitrary, values of 1 to 10 times the piezoelectric capacitance have been found suitable. To equate the frequencies of electrical and mechanical resonance, the inductor is tuned as follows:

$$L = \frac{C + C_p}{CC_p\omega_1}. \tag{11}$$

The resistance value, dependent on the inherent system damping, is most easily found experimentally. For such systems, resistances in the order of 1 $k\Omega$ are typical.

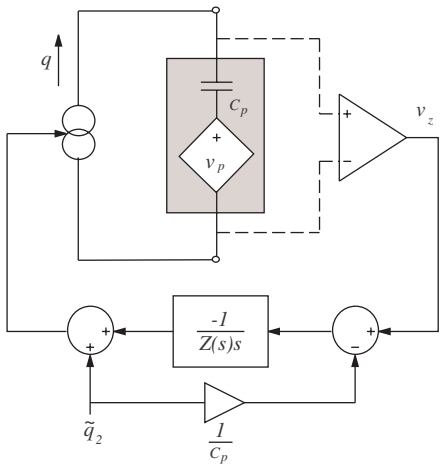

Fig. 6. Simplified implementation of a charge amplifier and piezoelectric shunt impedance.

III. Implementation

Resonant piezoelectric shunt damping circuits require impractically large values of inductance, typically in the tens of Henrys. For this reason the shunt damping circuit will be synthesized artificially using the charge amplifier. Consider the schematic shown in Figure 6. Neglecting the input q_2, the charge applied to the piezoelectric tube is equal to

$$q = v_z\frac{-1}{sZ(s)}. \tag{12}$$

The impedance (or admittance) experienced by the piezoelectric transducer can be calculated by examining the ratio of current to voltage at its terminals. As the current is equal to $-\dot{q}$, and q is defined by (12), the impedance presented to the terminals is simply $Z(s)$ (as defined by the filter in Figure 6). By implementing the filter $\frac{-1}{sZ(s)}$ any arbitrary impedance can be presented to the terminals of the transducer. Simple techniques for designing analog and digital filters that represent $\frac{1}{Z(s)}$ can be found in [16]. In this work a dSpace DSP system is used to implement and tune the filter $\frac{-1}{sZ(s)}$.

In addition to the charge required for shunt impedance synthesis, the additive charge q_2 is used for tube scanning. As mentioned in Section II-B, the additive charge q_2 requires a filter $F^{-1}(s)$ to compensate for the electrical dynamics of the shunt impedance when attached to the same electrode.

A substantial simplification can be made by studying the structure of the filter $F^{-1}(s)$,

$$F^{-1}(s) = \frac{1}{K(s)Z(s)} = \frac{1 + C_psZ(s)}{C_psZ(s)} = \frac{1}{C_psZ(s)} + 1. \tag{13}$$

Considering that the transfer function $\frac{1}{sZ(s)}$ has already been implemented, $F^{-1}(s)$ can be replaced as shown in Figure 6.

A. DC Accurate Charge Amplifier

One of the key components utilized without reference in the previous sections is the charge amplifier. As mentioned in the introduction, substantial difficulties have been revealed in attempts to construct such a device for capacitive loads.

A solution to the problem of voltage drift in charge amplifiers with capacitive loads was first presented in [17]. An auxiliary voltage feedback loop was included to correct

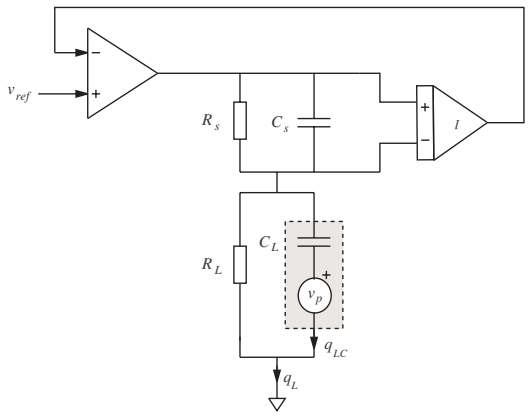

Fig. 7. DC accurate charge source for grounded capacitive loads.

low-frequency behavior and allow for constant charge offsets. The circuit implementation required the design of separate voltage and charge feedback controllers. A simplified design relying on the intrinsic voltage control offered by the parasitic resistances was later presented in [18]. Neither of the amplifiers discussed have been capable of driving grounded loads. As piezoelectric tubes have multiple external electrodes and a common (often grounded) internal electrode, the requirement for a grounded-load is a necessity.

Following we present the design of a DC accurate grounded-load charge amplifier. Shown in Figure 7, the amplifier incorporates a high common-mode rejection, high common-mode range differential stage consisting of the lower opamp, voltage bridge, and instrumentation amplifier. The amplifier works to equate the voltage measured across the sensing impedance to the reference voltage v_{ref}.

To understand the operation of the amplifier we study the transfer function from the reference voltage v_{ref} to the load charge q_{LC}.

$$\frac{q_L(s)}{v_{ref}(s)} = C_s \frac{s + \frac{1}{C_s R_s}}{s} \tag{14}$$

The transfer function from reference to actual load charge can be found by combining equation (14) with an expression relating q_L to q_{LC},

$$\begin{aligned} \frac{q_{LC}(s)}{v_{ref}(s)} &= \frac{q_L(s)}{v_{ref}(s)} \frac{q_{LC}(s)}{q_L(s)} \\ &= C_s \frac{s + \frac{1}{C_s R_s}}{s} \frac{s}{s + \frac{1}{R_L C_L}} \end{aligned} \tag{15}$$

By setting $C_L R_L = C_s R_s$, i.e.

$$\frac{R_L}{R_s} = \frac{C_s}{C_L} \tag{16}$$

the amplifier has no low frequency dynamics and constant gain $C_s\ Columbs/Volt$. Effectively the voltage amplifier, comprised of the two resistances R_L and R_s, synthesizes the operation of an ideal charge amplifier at low frequencies.

If the amplifier can be viewed as the concatenation of a voltage and charge amplifier, an important question is: in what regions of operation does the amplifier operate as a pure charge amplifier?, likewise for voltage operation. Consider the schematic shown in Figure 8. During perfect charge operation i.e., when q_{LC} is correctly regulated to zero, the voltage

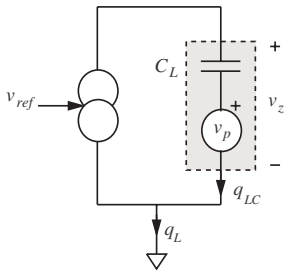

Fig. 8. Test for voltage / charge dominance.

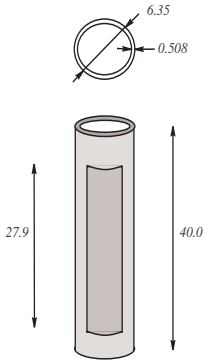

Fig. 9. Piezoelectric tube dimensions (in mm).

v_z will be equal to v_p. During voltage dominant behavior, v_z will be regulated to zero. Such characteristics can easily be measured experimentally. Although the voltage dynamics have been designed to perfectly synthesize the operation of an ideal charge amplifier, during voltage dominant operation, if the load is not purely capacitive, errors in q_{LC} will occur.

When $v_{ref} = 0$, which implies $q_L = 0$, the transfer function from v_p to v_z reveals the voltage or charge dominance of the amplifier. At frequencies where $v_z \approx v_p$, the amplifier is charge dominant, and voltage dominant when $v_z \approx 0$. For the hybrid amplifier shown in Figure 7, when $v_{ref} = 0$,

$$\frac{v_z(s)}{v_p(s)} = \frac{s}{s + \frac{1}{R_L C_L}} \tag{17}$$

i.e. at frequencies above $\frac{1}{RC}\ s^{-1}$ the amplifier is charge dominant, and voltage dominant below. Obviously, given equation (17), the objective will be to select a load resistor R_L as large as possible. This may be limited by other factors such as opamp current noise attenuation, bias-current based offset voltages, and the common-mode and differential leakage of the opamp. In practice $\frac{v_z(s)}{v_p(s)}$ is best measured by simply applying a voltage to another electrode and using that as a reference. As the frequencies under consideration are well below the tube's first mechanical resonance, the applied voltage will be related by a constant.

IV. Experimental Results

In this section, the prototype shunt circuit and charge amplifier are employed to drive a piezoelectric tube positioner in one dimension. Physical dimensions of the tube can be found in Figure 9. An ADE Tech capacitive sensor was used to measure the displacement with sensitivity $10\ V/\mu m$ and bandwidth $10\ kHz$. An aluminium cube ($1\ cm \times 1\ cm \times$

Charge Gain	77.8 nC/V
Voltage Measurement Gain	0.1 V/V
L	2.9 H
C	50 nF
R	3.3 $k\Omega$

TABLE I
PARAMETERS OF THE CHARGE AMPLIFIER AND SHUNT IMPEDANCE

1 cm) is glued onto the tube tip and grounded to provide a return for the capacitive sensor. Parameters of the shunt impedance and amplifier are shown in Table I.

The nominal first resonance frequency and DC charge sensitivity of the tube were measured to be 1088 Hz and 5.7 m/C (= 5.7 $\mu m/\mu C$).

A. Amplifier Performance

As discussed in Section III-A, the bandwidth of charge dominance was ascertained by zeroing the charge reference and introducing an internal load voltage. We observe a charge dominance bandwidth of 0.8 Hz. Frequencies above this bandwidth will experience the full linearity benefit of charge actuation.

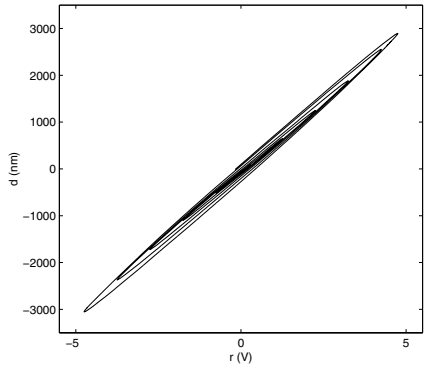

Fig. 10. Relationship between an applied voltage and the resulting tube displacement. (10 Hz ramped sinusoidal input).

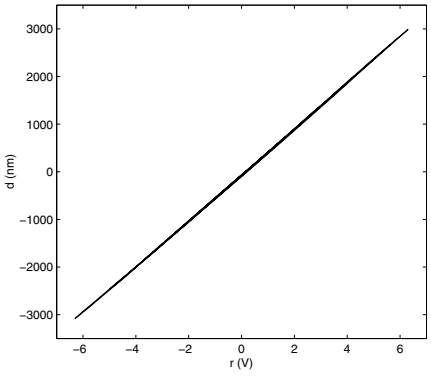

Fig. 11. Relationship between an applied charge reference and the resulting tube displacement. (10 Hz ramped sinusoidal input).

To justify the use of charge actuation we demonstrate the benefit in Figures 10 and 11. Hysteresis is reduced by approximately 89% simply through the use of a charge amplifier. Percentage reduction is calculated by measuring the maximum excursion in the minor axis of each plot, then taking the ratio $100 \times \frac{\text{voltage}}{\text{charge}}$. It should be noted that a scan

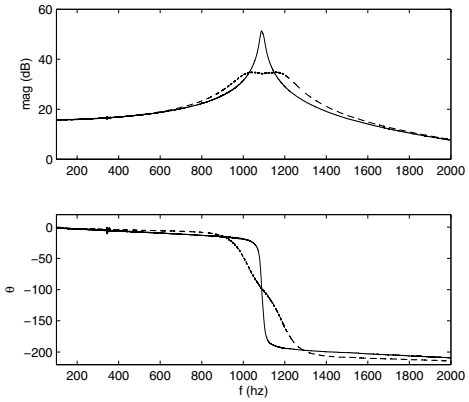

Fig. 12. Experimental Response. Natural (—) and shunt-damped (- -) tube dynamics measured from the additive charge input q_2 (C) to the tip displacement d (m).

range of ± 3 μm is around 20% of the full scale deflection, it is often assumed that hysteresis is negligible at such low drives. Similar plots for the same apparatus with a ± 8 μm drive can be found in [17], a greater hysteresis is exhibited, and heavily reduced through the use of a similar charge drive.

B. Shunt Damping Performance

Whilst scanning at high frequencies, the greatest cause of tracking error is excitation of the mechanical resonance. Such high frequency components can be reduced by filtering, or signal optimization in case of periodic scanning. Nevertheless, some residual excitation of the mechanical resonance is inevitable.

To illustrate the improvement in triangular scanning fidelity, an unfiltered 46 Hz triangular waveform was applied to the system. The frequency and lack of filtering was chosen to illustrate the worst-case induced ripple. In practice, the triangle would be filtered or passed through a feedforward controller to reduce vibration. Regardless of the ripple magnitude, the presence of a shunt circuit provides the same decrease in settling time. At high speeds, significant increases in fast-axis resolution can be expected. In the case where feedforward vibration control [19] is applied, the damped mechanical system would allow a less severe pre-filter and provide greater immunity to modeling error.

The influence of the shunt impedance can be observed to significantly increase the effective damping in Figure 12. Time domain improvements for a triangular scanning signal can be observed in Figure 13.

Another significant source of tracking error is external mechanical noise. Due to the highly resonant nature of the tube, high frequency noise components can excite the mechanical resonance and lead to large erroneous excursions. By applying a voltage to an opposite electrode, we can simulate the effect of a strain disturbance. A significant damping of the mechanical resonance by greater than 20 dB was observed. The time domain reduction of resonant vibration can be seen in Figure 14.

The final test of such an apparatus is the ability to track DC charge offsets. In Figure 15 a low frequency triangle signal was applied to the charge amplifier, at time 130 sec a DC offset equivalent to around 1 μm was applied. Aside from the faithful reproduction of a 0.1 Hz triangle wave, the charge amplifier reproduces the offset without drift.

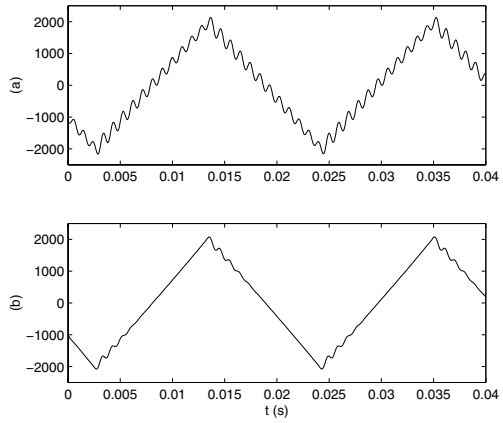

Fig. 13. Tube deflection (in nm) resulting from a 46 Hz triangle wave excitation. Uncontrolled (b), and with $L-C-R$ shunt impedance (a).

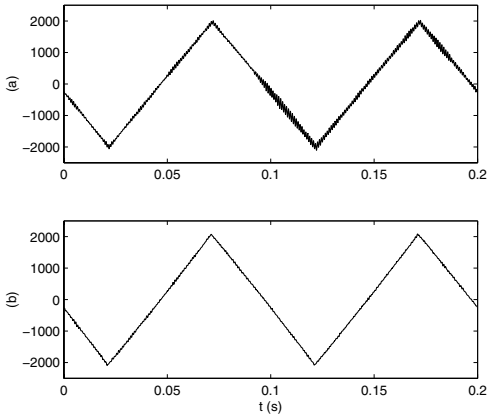

Fig. 14. Tube deflection (in nm) resulting from a 1.6 kHz bandlimited uniformly distributed random strain disturbance. Uncontrolled (b), and with $L-C-R$ shunt impedance (a).

V. Conclusions

In this paper, we have presented a new charge amplifier for reduction of hysteresis in piezoelectric tube actuators. Using the intrinsic voltage feedback offered by parasitic resistances, low-frequency voltage drift has been eliminated to provide DC accurate charge actuation. The proposed charge amplifier is simple to fabricate, and easily integrated into existing open-loop or controlled systems.

In addition to hysteresis reduction, a simple technique has been proposed for the reduction of vibration. Piezoelectric shunt damping involves the connection of an electrical impedance to the terminals of a piezoelectric transducer. In experiments considering scan-induced and externally-induced vibration, an LCR network reduces the first resonance frequency by 20 dB in magnitude. No feedback sensors are required.

Although charge driven shunt damped piezoelectric tubes can be integrated into previous design methodologies, the simplicity-of-implementation and achievable performance warrants their use independently.

Current work includes the design of an all-analog amplifier incorporating both charge actuation, and shunt impedance implementation.

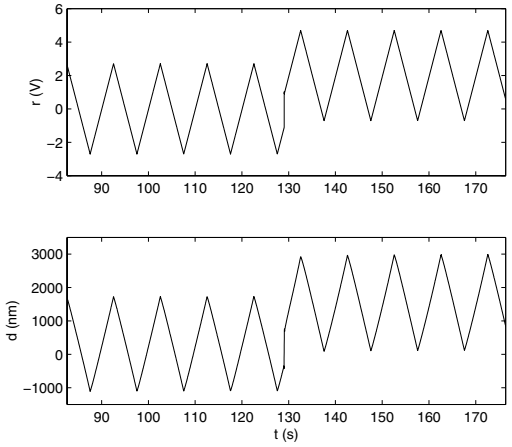

Fig. 15. Low frequency scanning reference and resultant tube displacement with additive DC offset.

References

[1] G. Binnig and D. P. E. Smith, "Single-tube three-dimensional scanner for scanning tunneling microscopy," *Review of Scientific Instruments*, vol. 57, no. 8, pp. 1688–1689, August 1986.

[2] D. Croft, D. McAllister, and S. Devasia, "High-speed scanning of piezo-probes for nano-fabrication," *Transactions of the ASME, Journal of Manufacturing Science and Technology*, vol. 120, pp. 617–622, August 1998.

[3] W. Gao, R. J. Hocken, J. A. Patten, J. Lovingood, and D. A. Lucca, "Construction and testing of a nanomachining instrument." *Precision Engineering*, vol. 24, no. 4, pp. 320–328, October 2000.

[4] I. of Electrical and E. E. Inc., "IEEE standard on piezoelectricity," ANSI/IEEE Std. 176–1987, 1988.

[5] C. J. Chen, "Electromechanical deflections of piezoelectric tubes with quartered electrodes." *Applied Physics Letters*, vol. 60, no. 1, pp. 132–134, January 1992.

[6] H. J. M. T. A. Adriaens, W. L. de Koning, and R. Banning, "Modeling piezoelectric actuators," *IEEE/ASME transactions on mechatronics*, vol. 5, no. 4, pp. 331–341, December 2000.

[7] C. V. Newcomb and I. Flinn, "Improving the linearity of piezoelectric ceramic actuators," *IEE Electronics Letters*, vol. 18, no. 11, pp. 442–443, May 1982.

[8] P. Ge and M. Jouaneh, "Tracking control of a piezoelectric actuator," *IEEE Transactions on control systems technology*, vol. 4, no. 3, pp. 209–216, May 1996.

[9] J. M. Cruz-Hernandez and V. Hayward, "Phase control approach to hysteresis reduction," *IEEE transactions on control systems technology*, vol. 9, no. 1, pp. 17–26, January 2001.

[10] H. Kaizuka and B. Siu, "simple way to reduce hysteresis and creep when using piezoelectric actuators," *Japan Journal of Applied Physics, Part 2 - Letters*, vol. 27, no. 5, pp. 773–776, May 1988.

[11] R. L. Forward, "Electronic damping of vibrations in optical structures," *Applied Optics*, vol. 18, no. 5, pp. 690–697, March 1979.

[12] N. W. Hagood and A. Von Flotow, "Damping of structural vibrations with piezoelectric materials and passive electrical networks," *Journal of Sound and Vibration*, vol. 146, no. 2, pp. 243–268, 1991.

[13] S. O. R. Moheimani, A. J. Fleming, and S. Behrens, "On the feedback structure of wideband piezoelectric shunt damping systems," *Smart Materials and Structures*, vol. 12, no. 1, pp. 49–56, February 2003.

[14] A. J. Fleming, "Synthesis and implementation of sensor-less shunt controllers for piezoelectric and electromagnetic vibration control," Ph.D. dissertation, The University of Newcastle, Callaghan 2308, Australia, February 2004.

[15] S. O. R. Moheimani, "A survey of recent innovations in vibration damping and control using shunted piezoelectric transducers." *IEEE Transactions on Control Systems Technology*, vol. 11, no. 4, pp. 482–494, July 2003.

[16] A. J. Fleming and S. O. R. Moheimani, "Improved current and charge amplifiers for driving piezoelectric loads, and issues in signal processing design for synthesis of shunt damping circuits." *Intelligent Material Systems and Structures*, vol. 15, no. 2, pp. 77–92, February 2004.

[17] ——, "hybrid DC accurate charge amplifier for linear piezoelectric positioning," in *Proc. 3rd IFAC Symposium on Mechatronic Systems*, Sydney, Australia, September 2004.

[18] K. A. Yi and R. J. Veillette, "A charge controller for linear operation of a piezoelectric stack actuator," *IEEE Transactions on Control Systems Technology*, vol. 13, no. 4, pp. 517–526, July 2005.

[19] D. Croft, G. Shed, and S. Devasia, "Creep, hysteresis, and vibration compensation for piezoactuators: Atomic force microscopy application," *Transactions of the ASME, Journal of Dynamic Systems, Measurement, and Control*, vol. 123, pp. 35–43, March 2001.